

Modeling of Fixed Bed Column Studies for Iron Removal from Industrial Effluents through Ion Exchange Process

Maria Dolores Víctor-Ortega, Javier Miguel Ochando-Pulido*, Antonio Martínez-Férez

Chemical Engineering Department, University of Granada, Avda. Fuentenueva s/n, 18071 Granada, Spain
 jmochandop@ugr.es

The performance of a fixed-bed cation exchange process was examined for final purification of the iron load derived from catalyst usage in the secondary treatment of olive mill wastewater, which led to unacceptable iron levels. Results showed an increase in the pH value up to 4 enhanced the iron IE efficiency, which decreased upon higher pH. Furthermore, Thomas model provided utmost accurate dynamic behavior modeling for all inlet concentrations studied (20, 50 and 100 mg L⁻¹).

1. Introduction

Contamination due to the presence of iron species can be found currently in natural waters (Ahmetli et al, 2007), mining effluents (Gaikwad, 2010), hydrometallurgical solutions (McKevitt and Dreisinger, 2009) and a range of other industrial wastes (Agrawal, 2009). In this sense, ion exchange (IE) and adsorption processes may be a potential solution for wastewater reclamation when metal ions are present in moderate levels in the effluent. IE is of particular interest since the metals can be potentially recovered, and the technology is simple and effective (Dabrowski et al., 2004). Compared with conventional separation and purification methods, IE provides several advantages involving lower operational costs, ease in handling, low consumption of reagents if properly optimized, as well as the possibility of recovering added-value components through desorption and regeneration of IE resins (Bulai and Cioanca, 2011; Abdel-Ghani et al., 2007).

In the present work, the performance of a fixed-bed IE process was addressed for the final purification of the iron load in a secondary-treated olive mill wastewater stream (OMW-2ST). Industrial effluents from olive oil industry are among the most recalcitrant and organic-polluted, up to a hundred times more than urban wastewaters, also presenting high saline toxicity. In previous work, the authors optimized and scaled-up a secondary treatment process for olive mill wastewater based on Fenton-like advanced oxidation, which successfully achieved high organic matter abatement efficiencies. However, the use of a ferric catalyst during the process leads to an increase of the iron concentration in the treated effluent exiting the Fenton-like reactor up to unacceptable levels (more than 14 mg L⁻¹) (Martínez-Nieto, 2010; European Commission, 1998).

Within this framework, continuous packed-bed column IE system may be a suitable and cost-efficient solution for the remediation of heavy metals in aqueous systems. Several studies can be found in the literature dealing with iron removal by means of strong acid-cation exchange resins (Kaya et al., 2002; Benítez et al., 2002; Marañón et al., 2005; Millar et al., 2015).

In the present research work, the performance of a fixed-bed IE process based on a strong-acid cation exchange resin was fully investigated. The influence of some key parameters on the IE performance and removal efficiency was elucidated, comprising the inlet concentration, the system pH and the equilibrium information related to the IE column breakthrough behavior, which provides information about the dynamic behavior of the metal concentration in time indispensable for appropriate column design (Guangyu, 2001; Viraraghavan et al., 2001). Column experiments were carried out to examine the breakthrough curves for different inlet iron concentrations. Moreover, the IE process was also modeled by fitting the experimental data to various adsorption models.

2. Materials and methods

2.1 Ion Exchange resin

The resin used in this research work was a strong-acid cation exchange resin (Dowex Marathon C), which was supplied by Sigma Aldrich. Firstly, the selected cation exchange resin was conditioned in HCl solution and finally in water before being used in the IE and desorption experiments, following the advice given by the resin manufacturer. The physical and chemical characteristics of the used resin are hereafter summarized in Table 1.

Table 1: Physico-chemical properties of Dowex Marathon C resin

Dowex Marathon C resin	
Type	Strong-acid cation
Matrix	Styrene-DVB, gel
Ionic form as shipped	H ⁺
Functional group	Sulfonic acid
Particle size, mm	0.55-0.65
Effective pH range	0-14
Total exchange capacity, eq L ⁻¹	1.80
Shipping weight, g L ⁻¹	800

2.2 Ion Exchange bench-scale plant

The IE column, set-up as fixed-bed, was made of an acrylic tube with dimensions 540 mm height x 46 mm internal diameter. A fixed amount of 69.2 g of the selected cation exchange resin was packed in the column, which resulted in 25.5 cm bed height of adsorbent. The desired effluent flow rate through the IE column could be adjusted and controlled by means of a peristaltic pump (Ecoline VC-380).

For the experiments, iron solutions were prepared by dissolving reagent-grade iron (III) chloride 30% (w/w) aqueous solution (provided by Panreac) in double distilled water. On the other hand, HCl 37 % solution, which was used in the regeneration process, was also provided by Panreac.

2.3 Ion Exchange bench-scale plant

Analytical grade reagents and chemicals with purity over 99 % were used for the analytical procedures, applied at least in triplicate. For the measurement of the total iron concentration, all iron ions were reduced to iron ions (II) in a thioglycolate medium with a derivative of triazine, forming a reddish-purple complex that was determined photometrically at 565 nm (Standard German methods ISO 8466-1 and German DIN 38402 A51) (Greenberg et al., 1992).

2.4 Inlet pH impact

The impact of the inlet pH (pH₀) on the IE performance for the final purification of the iron load in OMW-2ST was examined by varying the pH₀ values in the range 1 - 7, while maintaining the resin dosage constant (3.5 g L⁻¹). The flow rate and the temperature were fixed at 10 L h⁻¹ and room temperature (298 K), respectively, whereas the contact time was varied up to 60 min in order to reach equilibrium (V́ctor-Ortega, 2014).

IE equilibrium was examined by performing recirculation mode experiments with the goal of obtaining the key equilibrium parameters of total iron/H⁺ IE process. The extent of the IE equilibrium data of iron species was determined by measuring the residual total iron concentration in the liquid phase. Previously, aqueous solutions of this contaminant were put in contact with the IE resin until equilibrium was achieved.

The removal efficiency was determined by computing the sorption percentage with Eq.(1):

$$\% \text{ Sorption} = \frac{C_0 - C_e}{C_0} \times 100 \quad (1)$$

where C₀ and C_e are the initial and equilibrium iron concentration (mg L⁻¹), respectively.

2.5 Fixed-bed column studies

Fixed-bed studies were performed by pumping iron solutions with different concentration values equal to 20 mg L⁻¹, 50 mg L⁻¹ and 100 mg L⁻¹, at a flow rate of 10 L h⁻¹ through the IE column.

The amount of adsorbed iron was calculated on the basis of the difference between the inlet concentration (C₀) and outlet concentration (C_t). The IE efficiency of the cationic exchange fixed-bed column was evaluated by determining the breakthrough curves, which were represented as a function of treated volume in terms of normalized concentration, C_t/C₀, defined as the ratio of outlet iron concentration, C_t (mg L⁻¹) to inlet iron concentration, C₀ (mg L⁻¹). The experimental curves were mathematically modeled by means of non-linear regression, and the parameters were estimated using the MS Excel 2011 program.

The breakthrough time t_b is defined as the time required for the concentration of metal ions in the effluent to reach 5 % of the inlet concentration. Otherwise, the exhaustion time t_E makes reference to the time at which the concentration of metal ions in the effluent becomes 90 % of the feedstream concentration.

2.6 IE process modeling: breakthrough curves

The models, hereafter described in the following sections, were fitted to the experimental breakthrough curves by non-linear regression methods. The regression coefficient (R^2) was used to evaluate the fitting of the experimental data to the non-linearized forms of Thomas, Yoon-Nelson, and Clark equations, whereas the sum of the squares of the errors (SSE) calculated according to Eq. (2) served as an indicator of the goodness of the adjustment between the experimental data and predicted values of C/C_0 used for plotting the breakthrough curves:

$$SSE = (q_{e,exp} - q_{e,cal})^2 \quad (2)$$

where the subscripts 'calc' and 'exp' make reference to the calculated and experimental values, respectively, and n is the number of measurements.

The linearized form of the model is given by the following equation (Thomas, 1944):

$$\ln\left(\frac{C_0}{C_t} - 1\right) = \frac{K_{Th} q_0 M}{Q} - K_{Th} C_0 t \quad (3)$$

where K_{Th} ($\text{ml mg}^{-1} \text{min}^{-1}$) is the Thomas rate constant, q_0 (mg g^{-1}) is the equilibrium adsorbate uptake, Q (ml min^{-1}) is the flow rate; C_t is the concentration of metal ion at time t and C_0 is the initial metal ion concentration. On the other hand, the linearized model equation for a single-component system is represented by the following expression (Yoon and Nelson, 1984):

$$\ln\left(\frac{C_0}{C_t} - 1\right) = K_{YN} \cdot t - \tau \cdot K_{YN} \quad (4)$$

where K_{YN} (min^{-1}) is the Yoon–Nelson rate constant, τ is the time required for 50 % adsorbate breakthrough (min), and t is the sampling time (min), whereas C_t is the concentration of metal ion at time t and C_0 is the initial metal ion concentration.

Finally, the linearized form of the model is given by the following expression (Clark, 1987):

$$\ln\left[\left(\frac{C_t}{C_0}\right)^{n-1} - 1\right] = -rt + \ln A \quad (5)$$

where n is the Freundlich constant; r and A are the Clark model parameters.

3. Results and discussion

3.1 Fixed-bed column studies

The influence of the inlet value (pH_0) on iron IE efficiency is reported in Fig. 1. The adsorption of iron ions was studied at different pH values in the range 1 - 7.

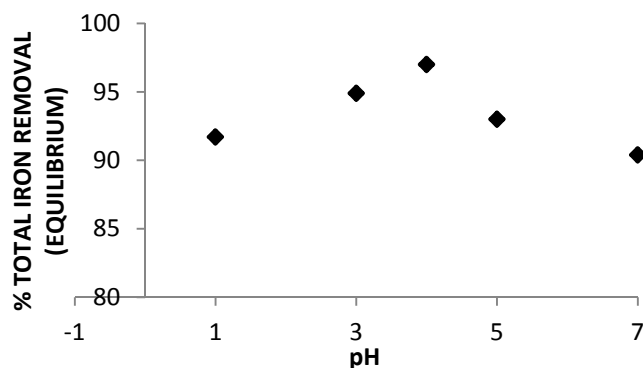


Fig. 1. Effect of pH on iron removal onto Dowex Marathon C resin (iron concentration = 50 mg L^{-1}).

As shown in Fig. 1, iron ions IE removal efficiency increased with an increase in the pH value up 4 but it can be observed that higher pH values led to lower IE efficiency. This is explained by the excessive protonation of the active sites of the selected strong-acid cation exchange resin at low pH values (below 4), which seems to hinder the formation of links between iron ions and the active sites of the cation exchange resin. Similar results were found by Senthil and Gayathri (2009) in their study on bael tree leaf powder as adsorbent to remove lead ions) from aqueous solutions. Moreover, at moderate pH_0 (3 - 5) the linked H^+ is released from the active sites of the cation exchange resin, and the extent of IE of iron ions is found to increase as a result of the acidification of the medium. However, further increasing the pH_0 , that is, above a value of 5, leads to decreased IE removal efficiencies, due to the fact that undesirable precipitation of metal hydroxides as dominant mechanism may yield reduced IE efficiency and hindrance of the cation exchange capacity.

In the column studies conducted by Rao et al. (2005) the solution pH was also noted to be an influential factor controlling the removal of iron from solution with a chelating IE resin. These authors observed that iron sorption efficiency decreased with increasing pH value on Duolite ES 467 resin. Approximately 30 % less iron was loaded on the resin at pH of 3 compared to pH equal to 2.

3.2 Breakthrough curves experiments

The IE efficiency of the fixed-bed strong-acid cation exchange column was evaluated by determining the breakthrough curves through column experiments at different inlet iron concentrations. In this case, mathematical models of Thomas, Clark and Yoon-Nelson in nonlinear forms were applied.

In our previous research works, a secondary treatment process for olive mill wastewater based on Fenton-like advanced oxidation was optimized and scaled-up, successfully achieving high organic matter abatement efficiencies. However, the use of a ferric catalyst during the process leads to an increase of the iron concentration in the effluent exiting the Fenton-like reactor up (OMW-2ST) to unacceptable levels (more than 14 mg L^{-1}) (Martínez-Nieto et al., 2010; European Commission, 1998). Moreover, these concentration values may become increased as a result of the fluctuations in the inlet concentrations of the olive mill effluent.

To cope with this fact, the effect of the initial iron concentration on the profiles of the breakthrough curves was examined in a fixed-bed column operating in continuous mode (Fig. 2), at constant flow rate and bed height.

Results show that increasing initial concentration values resulted in an earlier breakthrough curve. Moreover, the highest volume could be treated upon the lowest initial concentration. Integration of the area above the breakthrough curve was performed for the determination of the iron loading on the IE resin. The obtained results of the iron loading capacity values were equal to 31.80, 45.16 and $59.24 \text{ mg Fe g}^{-1}$ when the initial concentrations were set at 20, 50 and 100 mg L^{-1} , respectively. This increase in the IE capacity could be explained by the fact that a higher influent iron concentration results in a higher driving force for the transfer process to overcome the mass transfer resistance (XiaoFeng et al., 2014).

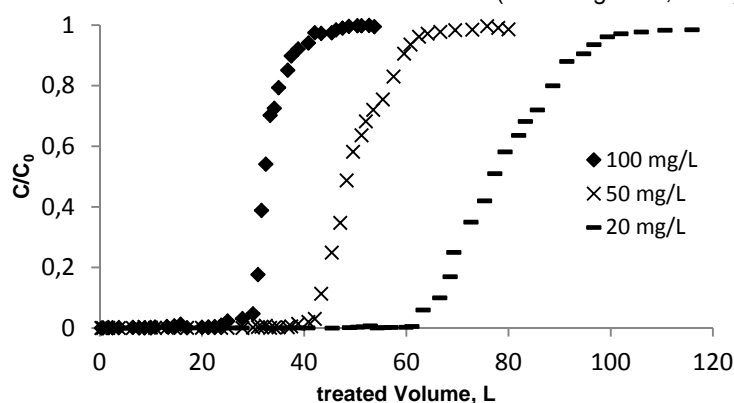


Fig. 2. Breakthrough curves for three different iron concentrations in the influent. Common conditions: flow rate = 10 L h^{-1} , resin amount = 69.2 g and operating temperature = 298 K .

The breakthrough curves are steeper with increasing pollutant concentrations. Similar results were also noticed by Hodaifa et al. (2014) for iron adsorption onto olive stones (at 5 and 20 mg L^{-1} iron concentration) and by Rao et al. (2005) for 50 and 100 mg L^{-1} in the treatment of wastewater containing Pb and Fe by IE. On the other hand, McKeivitt and Dreisinger (2009) demonstrated that a wide variety of resins gave rise to breakthrough curves comparable to the one shown in Fig. 2.

Table 2 shows the experimental t_B and the exhaustive capacities (q_{eq}) obtained for the different studied iron concentrations. It was observed that t_B decreased with increasing inlet iron concentration.

Table 2. Breakthrough times and exhaustive capacities for different inlet iron concentrations.

Inlet iron concentration (mg L^{-1})	t_B (min)	q_{eq} (mg g^{-1})
20	350	31.80
50	270	45.16
100	195	59.24

Thomas, Yoon-Nelson, and Clark equations were used to correlate the IE breakthrough curves' experimental data and model the adsorption process of iron on the selected resin, for proper dimension, operation and reliable scale-up. The values of the parameters obtained from the fitting of the experimental iron IE data to Thomas model are hereafter reported in Table 3, comprising mainly the Thomas rate constant K_{Th} together with the equilibrium adsorbate uptake q_0 .

Table 3: Thomas model parameters of iron ions adsorption onto Dowex Marathon C resin

Inlet iron concentration (mg L ⁻¹)	Thomas model parameters			
	k _{Th} (ml min ⁻¹ mg ⁻¹)	q ₀ (mg g ⁻¹)	R ²	SSE
20	0.075	22.16	0.9868	0.030
50	0.064	36.52	0.9476	0.107
100	0.058	48.23	0.9655	0.117

It was found that the values of q_0 estimated using the Thomas model are very close to the q_e values obtained from the experimental results with varying C_0 conditions. Comparing the R^2 and SSE values for various models revealed that the Thomas model described with utmost suitability the iron ions IE process in a fixed-bed column (Table 3). Otherwise, the results obtained from the modeling with Yoon-Nelson model are summarized in Table 4, where the estimated values of the Yoon-Nelson constant K_{YN} , the adsorption capacity q_0 , the 50 % adsorbate breakthrough τ , and additional statistical parameters are reported. In this case, the value of K_{YN} was noted to decrease with increasing the initial iron concentration in the effluent. Furthermore, the values of τ were found to be lower than the t value at 50 % breakthrough experimentally observed under all conditions assayed. These results demonstrate that Yoon-Nelson model is not very accurate in the prediction of the τ value. Finally, Clark model was applied for the performance modeling of the fixed-bed IE process for the final purification of the iron load in OMW-2ST (Table 5). The value of the Freundlich constant ($n = 1.64$), which was obtained from the batch tests in our previous work (V́ctor-Ortega et al., 2016), was used in the Clark model to calculate the other model parameters. As seen in Table 5, R^2 values were lower in comparison to the previous models examined, and the corresponding SSE values were calculated to be higher, indicating that the Clark model predicts worst the breakthrough curve of iron adsorption process among all tested model equations.

Table 4: Yoon-Nelson model parameters of adsorption of iron ions onto Dowex Marathon C resin

Inlet iron concentration (mg L ⁻¹)	Yoon and Nelson model parameters			
	K _{YN} (min ⁻¹)	τ (min)	q ₀ (mg g ⁻¹)	R ²
20	0.0313	504.8	24.31	0.8704
50	0.0313	288.7	34.77	0.9650
100	0.0465	198.2	47.74	0.9465

Table 5: Clark model parameters of adsorption of iron ions onto Dowex Marathon C resin

Inlet iron concentration (mg L ⁻¹)	Clark model parameters			
	r (min ⁻¹)	A	t _B (min)	R ²
20	0.0159	1079.9	330.60	0.8669
50	0.0159	347.48	257.17	0.8380
100	0.0213	106.18	181.73	0.8719

4. Conclusions

In the present work, the performance of a fixed-bed IE process with a strong-acid cation exchange resin was investigated for the final purification of the iron load in a secondary-treated olive mill wastewater stream (OMW-2ST). Results showed that optimal pH value was found to be 4. In addition, experimental data withdrawn from breakthrough curves demonstrated up to 59.24 mg g⁻¹ maximum iron adsorption capacity onto the selected strong-acid cation exchange resin. Moreover, the iron equilibrium uptake efficiency was observed to strikingly increase with the increment of the inlet iron ion concentration. Both the breakthrough point and the exhaustion time decreased with an increase of the inlet iron ion concentration. Furthermore, modeling of the proposed IE process was performed with utmost accuracy by means of Thomas model for all three inlet iron concentrations studied, providing the necessary information about the dynamic behavior of the iron IE process for appropriate column design and operation.

Acknowledgements

Spanish Ministry of Science and Innovation is acknowledged for funding the project CTQ2010-21411 and CTM2014-61105-JIN. The University of Granada is also sincerely acknowledged.

References

- Abdel-Ghani, N.T., Hefny, M., El-Chagbany, G.A.F. 2007. Removal of Lead (II) from aqueous solution using low cost abundantly available adsorbents. *Int. J. Environ. Sci. Tech.* 4(1), 67-73.
- Agrawal, A., Kumari, S., Sahu, K.K. 2009. Iron and copper recovery/removal from industrial wastes: a review. *Ind. Eng. Chem. Res.* 48 (13), 6145–6161.
- Ahmetli, G., Tarlan, E. 2007. Fe(II/III) adsorption onto styrene/divinyl benzene based polymers. *J. Appl. Polym. Sci.* 104(4), 2696–2703.
- Benítez, P., Castro, R., Barroso, C.G. 2002. Removal of iron, copper and manganese from white wines through ion exchange techniques: effects on their organoleptic characteristics and susceptibility to browning. *Anal. Chim. Acta* 458 (1), 197–202.
- Bulai, P., Cioanca, E. 2011. Iron removal from wastewater using chelating resin Purolite S930. *Tehnomus Journal* (18), 63 – 67.
- Clark, R.M. 1987. Evaluating the cost and performance of field-scale granular activated carbon systems, *Environ. Sci. Technol.* 21, 573–580.
- Dabrowski, A., Hubicki, Z., Podkoscielny, P., Robens, E. 2004. Selective removal of the heavy metal ions from waters and industrial wastewaters by ion-exchange method. *Chemosphere* 56 (2), 91–106.
- European Commission. 1998. Council Directive 98/83/EC of 3 November 1998 on the quality of water intended for human consumption. Brussels, Belgium.
- Gaikwad, R.W. 2010. Review and research needs of active treatment of acid mine drainage by ion exchange. *Electron. J. Environ. Agric. Food Chem.* 9, 1343–1350.
- Greenberg, A.E., Clesceri, L.S., Eaton, A.D. 1992. *Standard Methods for the Examination of Water and Wastewater*, APHA/AWWA/WEF, 16th ed., Washington DC. Cabs.
- Guangyu, Y., Viraraghavan, T. 2001. Heavy metal removal in a biosorption column by immobilized *M. rouxii* biomass. *Bioresour. Technol.* 78, 243–249.
- Hodaifa, G., Alami, S.B.D., Ochando-Pulido, J.M., Víctor-Ortega, M.D. 2014. Iron removal from liquid effluents by olive stones on adsorption column: breakthrough curves. *Ecol. Eng.* 73, 270-275.
- Kaya, Y., Vergili, I., Acarbabacan, S., Barlas, H. 2002. Effects of fouling with iron ions on the capacity of demineralization by ion exchange process. *Fresenius Environ Bull* 11, 885–888.
- Marañón, E., Fernández, Y., Castrillón L. 2005. Ion exchange treatment of rinse water generated in the galvanizing process, *Water Environ. Res.* 77(7), 3054–3058.
- Martínez Nieto, L., Hodaifa, G., Rodríguez Vives, S., Giménez Casares, J.A. 2010. Industrial plant for olive mill wastewater from two-phase treatment by chemical oxidation. *J. Environ. Eng.* 136 (11), 1309-1313.
- McKeivitt, B., Dreisinger, D. 2009. A comparison of various ion exchange resins for the removal of ferric ions from copper electrowinning electrolyte solutions part I: electrolytes containing no other impurities. *Hydrometallurgy* 98 (1–2), 116–121.
- Millar, G.J., Schot, A., Couperthwaite, S.J., Shilling, A., Nuttall, K., de Bruyn, M. 2015. Equilibrium and column studies of iron exchange with strong acid cation resin, *J. Environ. Chem. Eng.* 3, 373–385.
- Rao, K.S., Dash, P.K., Sarangi, D., Chaudhury, G.R., Misra, V.N. 2005. Treatment of wastewater containing Pb and Fe using ion-exchange techniques. *J. Chem. Technol. Biotechnol.* 80 (8), 892–898.
- Sag, Y., Yalcuk, A., Kutsal, T. 2001. Use of a mathematical model for prediction of the performance of the simultaneous biosorption of Cr(VI) and Fe(III) on *Rhizopus arrhizus* in a semi-batch reactor. *Hydrometallurgy* 59, 77–87.
- Senthil Kumar, P., Gayathri, R. 2009. Adsorption of Pb²⁺ ions from aqueous solutions onto bael tree leaf powder: isotherms, kinetics and thermodynamics study, *J. Eng. Sci. Technol.* 4 (4), 381-399.
- Thomas, H.C. 1944. Heterogeneous ion exchange in a flowing system. *J. Am. Chem. Soc.* 66, 1664–1666.
- Víctor-Ortega, M.D., Ochando-Pulido, J.M., Godaifa, H., Martínez-Férez, A. 2014. Final purification of synthetic olive oil mill wastewater treated by chemical oxidation using ion exchange: Study of operating parameters. *Chem. Eng. Process* 85, 241-247.
- Víctor-Ortega, M.D., Ochando-Pulido, J.M., Martínez-Férez, A. 2016. Thermodynamic and kinetic studies on iron removal by means of a novel strong-acid cation exchange resin for olive mill effluent reclamation. *Ecol. Eng.* 86, 53-59.
- XiaoFeng, S., Tsuyoshi, I., Masahiko, S., Takaya, H., Koichi, Y., Ariyo, K., Shiori, N. 2014. Adsorption of phosphate using calcined Mg₃-Fe layered double hydroxides in a fixed-bed column study. *J. Ind. Eng. Chem.* 20, 3623-3630.
- Yoon, Y.H., Nelson, J.H. 1984. Application of gas adsorption kinetics. I. A theoretical model for respirator cartridge service time. *Am. Ind. Hyg. Assoc. J.* 45, 509–516.